Limnol. Oceanogr., 47(1), 2002, 95–107

Contribution of absorption and scattering to the attenuation of UV and photosynthetically available radiation in Lake Biwa

Claude Belzile[1] *and Warwick F. Vincent*
Département de biologie et Centre d'études nordiques, Université Laval, Sainte-Foy, Québec, GIK 7P4, Canada

Michio Kumagai
Lake Biwa Research Institute, 1-10 Uchidehama, Otsu, Japan

Abstract

Underwater ultraviolet (UV) attenuation is typically modeled using correlative relationships between UV attenuation and dissolved organic carbon (DOC) concentration or colored dissolved organic matter (CDOM) absorption. Our objective was to validate and extend a biogeooptical model of UV penetration that would take into account total absorption as well as scattering by all components of the water column. Diffuse attenuation coefficients, $K_d(\lambda)$, for photosynthetically available radiation (PAR) and UV irradiance were measured using a PUV500 radiometer at 13 stations in Lake Biwa, Japan, in late summer. Absorption, *a*, and scattering, *b*, were measured at nine PAR wavelengths using an AC-9 absorption-attenuation meter. The average K_d(PAR) through the euphotic zone, K_{dav}(PAR), was estimated from the measured inherent optical properties using Kirk's equations derived from Monte Carlo simulations. The modeled K_{dav}(PAR) was strongly correlated with measured K_d(PAR) values ($r^2 = 0.998$), although the model systematically underestimated measured values by ≥15%. The relative contribution of absorption and scattering to UV attenuation was evaluated from measurements of the absorption coefficients, an extrapolation of *b* into the UV, and Kirk's equations. The UV-absorption coefficients for CDOM and particulate matter were measured spectrophotometrically. There was a close agreement between modeled and measured K_d(UV) values ($r^2 \geq 0.990$). The Lake Biwa data showed that particulate absorption and scattering play significant roles in UV attenuation; on average, absorption by water, CDOM, and particles contributed 1, 66, and 21% respectively to K_{dav}(340), while scattering by particles contributed 11%. At a turbid site (NS9) absorption by water, CDOM, and particles contributed 0.3, 40, and 36% respectively to K_{dav}(340), while scattering contributed the remaining 24%. The model described here integrates the effects of all absorption as well as scattering components and provides a more accurate estimate of underwater UV exposure than previous approaches based on CDOM absorption only.

Dissolved organic carbon (DOC) is often the major factor explaining among-lake variability in ultraviolet (UV) attenuation (Scully and Lean 1994; Morris et al. 1995; Laurion et al. 1997; Vincent et al. 1998), and this relationship appears to be due to the strong UV absorption by colored dissolved organic matter (CDOM). Different models have been established to relate UV attenuation to DOC or a_{CDOM} (*see Table 1* for symbols and units) and have been applied in modeling studies (e.g., Pienitz and Vincent 2000). However, these empirical correlative models are site-specific and their predicted K_d(UV) values can differ significantly for the same DOC or a_{CDOM}.

Recently, several authors reported substantial deviations from previously published UV-attenuation models (Hodoki and Watanabe 1998; Smith et al. 1999; Laurion et al. 2000). These deviations have been attributed to significant attenuation caused by scattering (Smith et al. 1999) or by absorption by particulate components (Hodoki and Watanabe 1998; Laurion et al. 2000). There has been little attempt, however, to relate such effects in a quantitative way to inherent optical properties.

The present study was undertaken to evaluate the role of scattering versus absorption for the attenuation of underwater UV with comparative measurements in the photosynthetically available radiation (PAR) waveband. Specifically, our objectives were (1) to partition underwater UV attenuation into its scattering and absorption components and (2) to estimate from simultaneous measurements of K_d, *a*, and *b*, the accuracy of Kirk's equations that are based on Monte Carlo simulations (Kirk 1984, 1991, 1994*a*). We undertook this study in Lake Biwa, Japan, which offers a broad range of optical conditions within a single water body and relatively low DOC. Preliminary studies on this lake showed that the diffuse attenuation coefficients for UV correlated with transmissometer measurements of the beam attenuation coefficient (*c*) at 660 nm (Vincent et al. 2001). These observations suggested that particles could play a significant role in UV attenuation and that this lake would be an appropriate system for developing a general model that incorporated scattering as well as absorption.

Methods

Sampling—Lake Biwa, Japan, is located in the midlatitude temperate zone (35°20′N, 136°10′E). With an area of 670 km^2, Lake Biwa is the largest lake in Japan, and its water

[1] Corresponding author (claude.belzile@bio.ulaval.ca).

Acknowledgments

This research was funded by the Natural Sciences and Engineering Research Council of Canada, the Fonds pour la Formation de Chercheurs et l'Aide à la Recherche of Quebec, the Centre d'études nordiques, and the Japan Science and Technology Agency. We thank Kanako Ishikawa, Ross F. Walker, Chunmeng Jiao, and the crew of the RV *Hakken* for the valuable help they provided in the field, and two anonymous reviewers for insightful suggestions.

Table 1. Notation List.

a	Absorption coefficient, m^{-1}
b	Scattering coefficient, m^{-1}
$\beta(\theta)$	Volume scattering function, m^{-1} sr^{-1}
c	Attenuation coefficient, m^{-1}
$E_d(z)$	Downward irradiance at depth z, μmol photons m^{-2} s^{-1} (for PAR) or μW cm^{-2} nm^{-1} (for UV)
$G(\mu_o)$	Coefficient determining the relative contribution of scattering to the vertical attenuation of irradiance
K_d	Vertical attenuation coefficient for downward irradiance, m^{-1}
K_{dav}	The average value of $K_d(\lambda)$ throughout the euphotic zone (from the surface to z_{eu}), m^{-1}
S	Slope parameter of the CDOM absorption curve, nm^{-1}
μ_o	Cosine of the zenith angle of refracted solar photons (direct beam) just beneath the surface
n	Exponent expressing the λ^{-n} dependence of b (λ)
SZA	Solar zenith angle, degrees
z_{eu}	Depth where downward irradiance is reduced to 1% of subsurface value, m

quality is a major concern since it is used for drinking, industrial, and agricultural purposes by more than 13 million people. The northern portion of the lake, the North Basin, has a mean depth of 44 m, is monomictic, and accounts for 90% of the total lake area. The South Basin has a mean depth of 3.5 m, is polymictic, and contains large populations of bloom-forming cyanobacteria in late summer.

Optical and biological measurements were made between 30 August and 5 September 2000 at 13 stations selected to encompass large variations in optical characteristics (Table 2). All sampling was done within 3 h of local noon, during clear sky or high diffuse clouds conditions. Water samples were collected at 0.5-m depth using a Niskin bottle and transferred immediately to dark polyethylene bottles. Samples were kept at 4°C until filtration (within 10 h). The seston was filtered onto GF/F filters for chlorophyll *a* (Chl *a*) determination following Nusch (1980) and on precombusted weighed GF/F filters for determination of total suspended solids (TSS) by weight.

Particulate absorption coefficient—Water samples were vacuum filtered in duplicate through a 25-mm GF/F filter, and the filters then stored at −20°C until measurement (within 2 weeks) of spectral absorption by particulate matter (a_p) using the quantitative filter technique (QFT). The absorbance of particles concentrated onto the filters was measured every 2 nm over the spectral range 320–820 nm according to Roesler (1998) using a Hewlett-Packard 8452A diode array spectrophotometer equipped with an integrating sphere (Labsphere RSA-HP-84). Below 320 nm, the signal-to-noise ratio became too low and absorbance could not be determined accurately. Absorbance values were converted to a_p using the algorithm of Roesler (1998). The replicates differed from the mean by at most 10%; the values presented below are averages for the two replicates.

CDOM absorption coefficient—The absorption coefficient for colored dissolved organic matter, a_{CDOM} (m^{-1}), was measured in samples that were filtered through prerinsed 0.22 μm Sartorius cellulose acetate filters immediately after collection and stored at 4°C in acid-cleaned, amber glass bottles until analysis (within 2 weeks). a_{CDOM} was measured every 2 nm over the wavelength (λ) range 250–820 nm using a 1-cm, acid-cleaned, quartz cuvette in a Hewlett Packard 8452A diode array spectrophotometer. Because of the low absorption encountered at most stations, the 1-cm cuvette did not allow for accurate measurement of a_{CDOM} at longer PAR wavelengths. Measurements were therefore restricted to the range 290–484 nm and fitted to the equation

$$a_{CDOM}(\lambda) = a_{CDOM}(\lambda_0)\exp(-S(\lambda - \lambda_0)) \quad (1)$$

where λ_0 is a reference wavelength and S is the slope parameter. This equation with the fitted parameters was then used to calculate a_{CDOM} over the range 290–700 nm. The S values are given in Table 2.

Table 2. Description of sampling sites in Lake Biwa. Date and time of optical measurements, solar zenith angle (SZA), μ_0 for PAR, water depth (z, m), chlorophyll *a* (Chl *a*, μg L^{-1}), total suspended solids (TSS, mg L^{-1}), CDOM absorption coefficient at 320 nm ($a_{CDOM}(320)$, m^{-1}), and slope parameter of $a_{CDOM}(290–484)$ (S, nm^{-1}).

Site	Date	Time	SZA	μ_0	z	Chl *a*	TSS	$a_{CDOM}(320)$	S
North Basin stations									
Nagahama	1 Sep 2000	1030	34.3	0.906	3.3	2.1	5.5	3.23	0.015
EW2	1 Sep 2000	1125	28.5	0.933	3.7	2.6	1.3	1.20	0.017
EW4	1 Sep 2000	1200	27.4	0.938	20.5	1.4	0.9	1.18	0.016
EW6	1 Sep 2000	1300	30.6	0.924	60.0	1.7	0.8	0.90	0.019
EW8	1 Sep 2000	1415	41.2	0.869	97.0	2.4	1.3	1.10	0.017
NS1	4 Sep 2000	1105	31.3	0.921	29.0	1.8	1.1	0.85	0.023
NS3	4 Sep 2000	1215	28.7	0.932	82.0	2.0	1.2	0.95	0.022
NS5	4 Sep 2000	1335	35.8	0.898	71.0	1.5	1.0	1.11	0.020
NS7	4 Sep 2000	1450	48.1	0.828	52.0	1.8	1.1	0.95	0.022
South Basin stations									
Akanoi Bay	30 Aug 2000	1050	30.8	0.923	2.1	7.6	11.8	6.90	0.012
NS9	5 Sep 2000	0945	42.2	0.863	3.4	4.4	13.5	2.30	0.017
NS10	5 Sep 2000	1035	34.6	0.904	2.9	3.3	3.3	2.32	0.017
HamaOtsu	5 Sep 2000	0905	49.2	0.822	3.2	3.3	2.5	2.23	0.017

In situ measurements of a and c—Absorption, a, and attenuation, c, were measured using an AC-9 (WET Labs) absorption-attenuation meter. The AC-9 measured a and c at wavelengths 412, 440, 488, 510, 532, 555, 650, 676, and 715 nm. After submerging the instrument and supplying power, the AC-9 was allowed to warm up for ~5 minutes. Data were then recorded for ~2 minutes at 0.5 m and a profile was made to ~25-m depth. The instrument was brought again to 0.5-m depth and data were recorded for another ~2 minutes. Average a and c at 0.5 m were calculated from data recorded before and after the profile. Measured a and c were corrected for pure water absorption and scattering following WET Labs recommendations. Pure water calibration was performed after each sampling day and varied only within the instrument precision (0.005 m^{-1}). The values of $a(715)$ were corrected for the temperature dependence of absorption according to Pegau et al. (1997), and values of $a(\lambda)$ were corrected for the scattering error of the absorption tube according to Zaneveld et al. (1994).

Water column diffuse attenuation coefficients—Downwelling, cosine-corrected UV (at λ = 305, 320, 340, and 380 nm) and PAR (400–700 nm) profiles were measured using a PUV500 radiometer (Biospherical Instruments). Profiles were made from the stern of the ship oriented toward the sun. Only the diffuse component of the global irradiance was affected by the ship shadow because the sun was kept within ±30° of the back of the ship during measurements. Irradiance profiles were recorded from the surface to 25 m (or to the bottom at shallower stations). Underwater irradiance measurements were corrected for dark current measured by fitting the radiometer with a light-tight Neoprene cap, at in situ temperature. An approximation of the average $K_d(\lambda)$ in the euphotic zone, $K_{dav}(\lambda)$, was determined by linear regression of the natural logarithm of $E_d(\lambda, z)$ versus depth. Because a deep Chl a–maximum was located close to the thermocline (~10 m), the $K_d(\lambda)$ determination was restricted to the epilimnion, where little variation of a and c as measured using the AC-9 was observed (Fig. 1). At each UV wavelength, the maximum depth considered was approximately equal to the depth where 1% of subsurface irradiance at that wavelength remained, except for 380 nm irradiance at Sta. EW2 and NS10 where 5 and 10% remained at the bottom of these respective water columns. At the deep stations of the North Basin, because the K_d determinations were restricted to the homogenous epilimnion, 5–11% of subsurface E_d(PAR) remained at the maximum depth considered; at the shallow stations, 6–26% of subsurface E_d(PAR) remained at the maximum depth considered.

Overview of the Kirk model—From Monte Carlo computer simulations, Kirk (1984, 1991, 1994*a*) showed that the average value of the vertical attenuation coefficient for downward irradiance in the euphotic zone, K_{dav}, can be expressed as an explicit function of a, b, and μ_0

$$K_{dav} = 1/\mu_0[a^2 + G(\mu_0)ab]^{0.5} \quad (2)$$

where a is the absorption coefficient, b is the scattering coefficient, μ_0 is the average cosine of the angle of the stream of photons just under the surface (calculated from the incident zenith angle using Snell's Law), and $G(\mu_0)$ is a function that specifies the relative contribution of scattering to vertical attenuation and whose value is determined by the shape of the volume scattering function, $\beta(\theta)$ and by μ_0. Kirk (1991) showed that, when considering K_{dav}, $G(\mu_0)$ can be related to μ_0 according to

$$G(\mu_0) = (g_1\mu_0 - g_2) \quad (3)$$

where g_1 and g_2 are numerical constants that vary with the volume scattering function used in the calculations. The classic Petzold's measurements of $\beta(\theta)$ at 530 nm have been made for waters with scattering coefficients varying over a factor of 50. The resulting $\beta(\theta)$ are very similar, having a standard deviation within 30% of the mean (Gordon 1989). Moreover, these $\beta(\theta)$ differ principally in their scattering at angles >25° (Gordon 1989), while most scattering in natural waters is at small forward angles. Kirk (1991) tabulated the values of g_1 and g_2 for 12 water types of varying scattering coefficient and $\beta(\theta)$. When $\beta(\theta)$ from the San Diego Harbor was used in the simulation, $G(\mu_0)$ varied from 0.235 to 0.157 for solar zenith angle (SZA) varying from 1 to 50°.

Kirk's equations have been previously used to estimate a and b from underwater irradiance diffuse attenuation and reflectance measurements (e.g., Weidemann and Bannister 1986; Shooter et al. 1998). However, to our knowledge, there have been no previous attempts using Kirk's equations to model K_{dav} from measured a and b and to compare modeled and measured K_{dav} in the PAR and UV wavebands.

Comparison of modeled and measured $K_{dav}(\lambda)$—The accuracy of Kirk's equations to describe $K_{dav}(\lambda)$ in Lake Biwa was first estimated for PAR. Since the AC-9 measures a_{Total} minus the absorption by pure water, the values for a_w (Pope and Fry 1997) and b_w (Buiteveld et al. 1994) were added to the inherent optical properties (IOPs) measured by the instrument. Solar zenith angle (SZA) was calculated from date, time, and latitude using equations given in Kirk (1994*b*); μ_0 was calculated from the SZA using Snell's Law, with the appropriate index of refraction for water and air at each wavelength. The values of $G(\mu_0)$ were calculated using Eq. 3 with values of g_1 and g_2 for three different $\beta(\theta)$ selected to represent the range of b measured in Lake Biwa (water types 1, 8, and 9 as described in Kirk 1991). The average value of the vertical attenuation coefficient for downward irradiance throughout the euphotic zone was calculated using Eq. 2. To allow comparison with the measured K_d(PAR), modeled $K_{dav}(\lambda)$ values were adjusted for the shape of in situ spectral distribution of E_d(PAR) and spectral $K_{dav}(\lambda)$ was integrated over the PAR range according to

$$K_{dav}(\mathrm{PAR}) = -z^{-1}\ln\left[\frac{\int_{400}^{700} E_d(0^-, \lambda)\exp[-K_{dav}(\lambda)z]\, d\lambda}{\int_{400}^{700} E_d(0^-, \lambda)\, d\lambda}\right] \quad (4)$$

where z is the depth at which PAR is attenuated to 1% of the subsurface value and $E_d(0^-, \lambda)$ is the downwelling PAR irradiance just below the water surface (Morel 1988). Be-

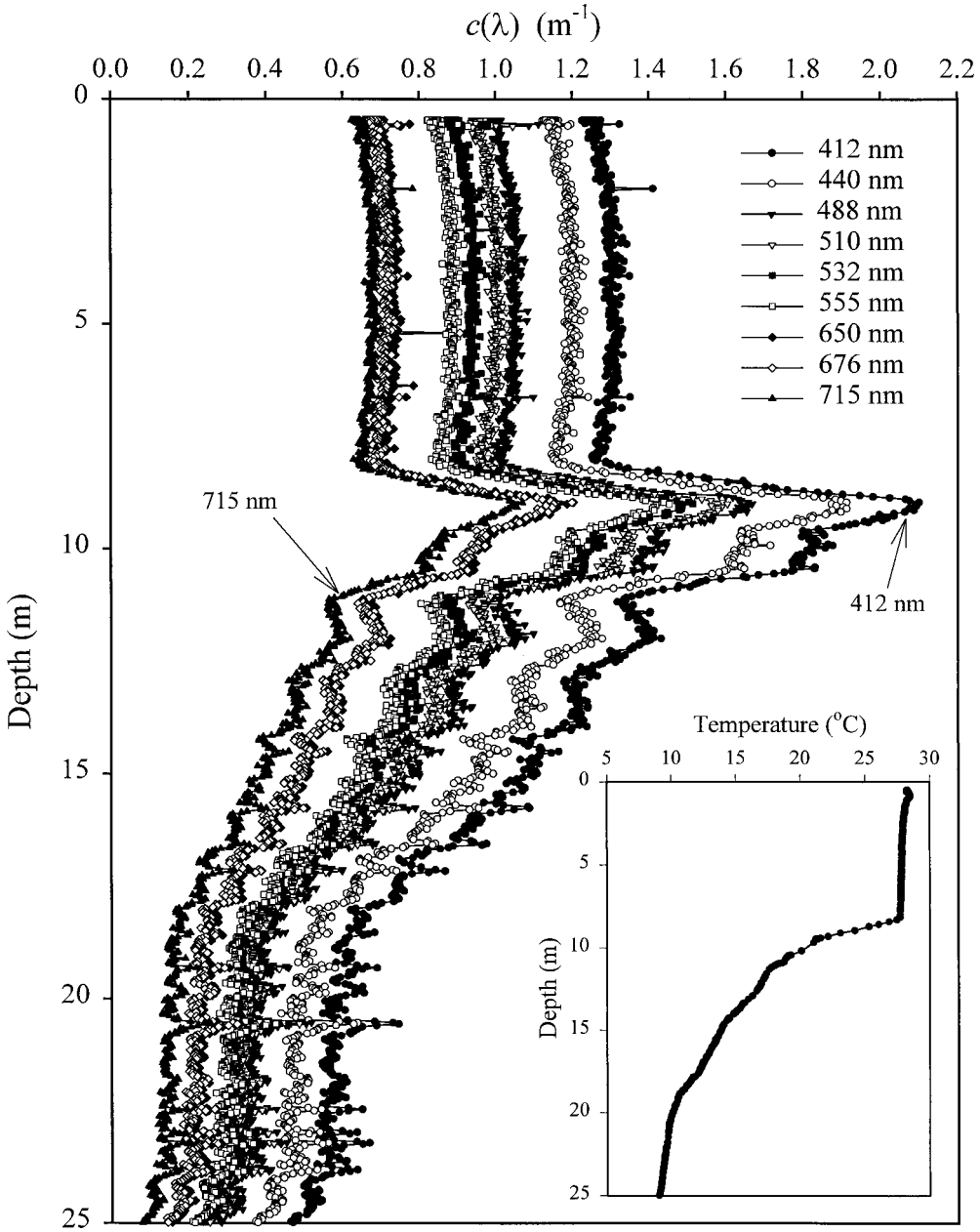

Fig. 1. Profile of the attenuation coefficient, $c(\lambda)$, measured using an AC-9 at Sta. EW6 in the South Basin of Lake Biwa, Japan. The insert shows the temperature profile measured using the PUV500.

cause $E_d(0^-, \lambda)$ was not measured in this study, we used the average spectrum for cloud-free sky and SZA $<45°$ presented by Morel (1988, his fig. 8). The integrated value of K_{dav}(PAR) is not very sensitive to the shape of $E_d(0^-, \lambda)$; using a flat spectrum instead of Morel's spectrum would change K_{dav}(PAR) by less than 1%.

Since a good agreement between measured and modeled K_{dav}(PAR) was found (*see Results*), Kirk's equations were then applied to UV irradiance at 320, 340, and 380 nm. $a_{CDOM}(\lambda)$ and $a_p(\lambda)$ in the UV waveband were measured by spectrophotometry and summed to obtain a_{spec}, which is equivalent to the absorption measured by the AC-9. The model was not applied at 305 nm because a_p could not be determined accurately for $\lambda < 320$ nm with the spectrophotometer. Pure water values from Buiteveld et al. (1994) were added to a_{spec} to obtain the total absorption coefficient. The scattering coefficient was extrapolated into the UV range (b_{ex}) from the AC-9 measurements over the wavelength range 412–676 nm. Spectral scattering was described using the relationship $b(\lambda) = a\lambda^{-n}$ where n is the usual exponent expressing the spectral dependency. This function gave an excellent fit to the data, with $r^2 > 0.93$ in all cases. Pure water values of b provided by Buiteveld et al. (1994) were added to b_{ex} to obtain the total scattering coefficient.

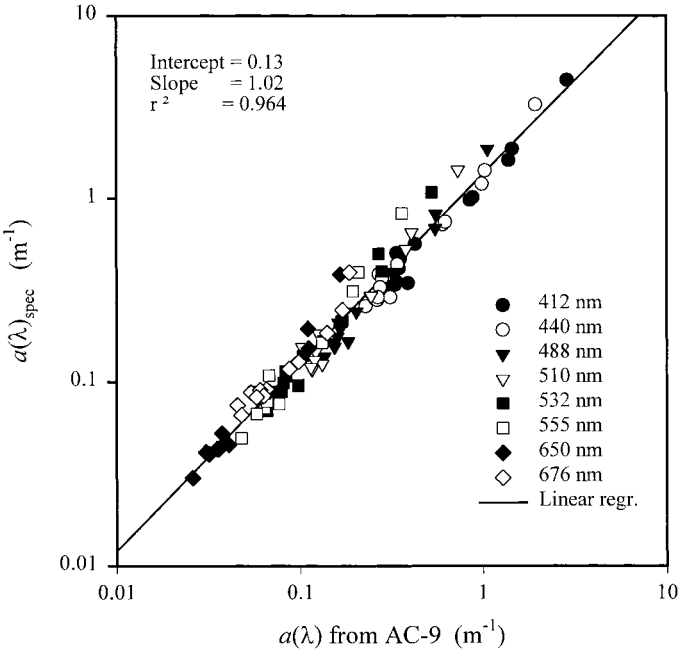

Fig. 2. Relationship between absorption coefficients for all wavelengths determined with the AC-9 at 0.5-m depth and those determined spectrophotometrically (a_{spec}, the sum of a_{CDOM} and a_p).

To examine the relative contribution of scattering and absorption by the dissolved and particulate fractions, $K_{dav}(\lambda)$ was computed using Eqs. 2 and 3 under three optical conditions:

Model I: Absorption by water and CDOM, no scattering by particles [$a = a_w + a_{CDOM}$ and $b = b_w$].

Model II: Absorption by water, CDOM, and particles, but no scattering by particles [$a = a_w + a_{CDOM} + a_p$ and $b = b_w$].

Model III: Absorption by water, CDOM, and particles, plus scattering by particles and water [$a = a_w + a_{CDOM} + a_p$ and $b = b_w + b_{AC\text{-}9}$]. For modeling K_{dav}(UV) from Eq. 2, $b_{AC\text{-}9}$ was replaced by b_{ex}.

Results

PAR absorption at specific wavelengths—There was excellent agreement between the absorption measured by the AC-9 and the sum of $a_{CDOM}(\lambda)$ and $a_p(\lambda)$ measured spectrophotometrically (Fig. 2). For the data pooled from all sites, the correlation coefficient was +0.96, the slope was approximately 1.0, and the intercept was small (not significantly different from zero). The generally close agreement between the two measurements of a is further illustrated for the full PAR spectrum at four optically contrasting sites (Fig. 3). Stations NS5 and EW6 (Fig. 3A,B) are typical of the clear waters of the North Basin and had low (<0.4 m^{-1}) values

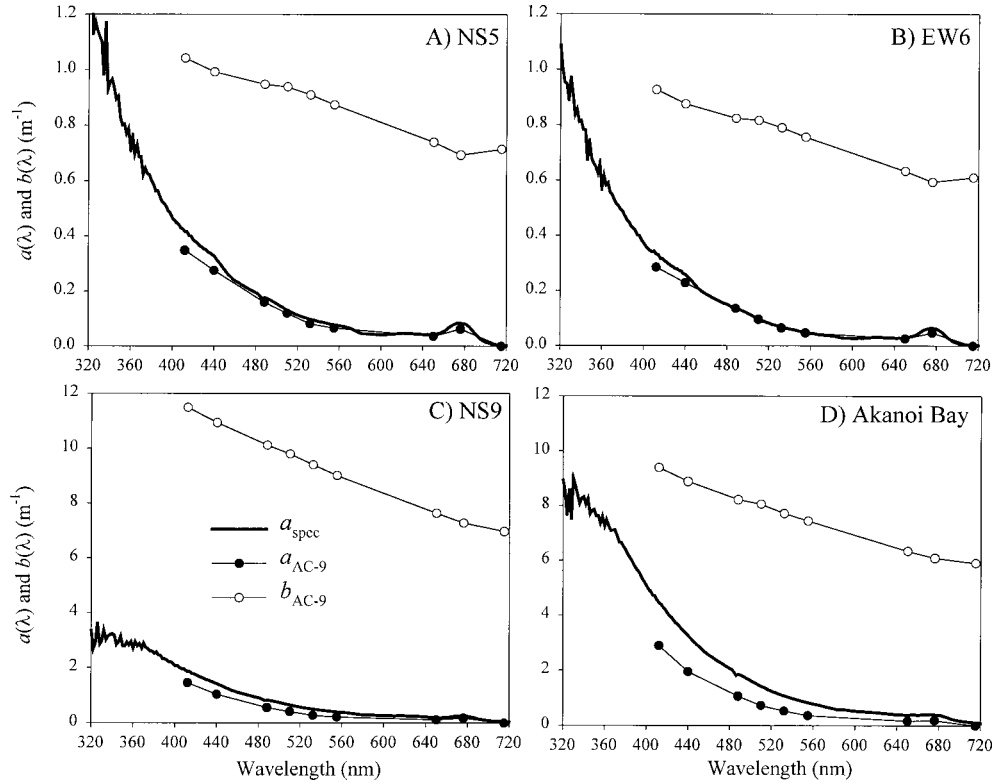

Fig. 3. Spectral absorption, $a(\lambda)$, and scattering, $b(\lambda)$, measured using an AC-9, and a_{spec}, the sum of a_{CDOM} and a_p measured spectrophotometrically. The four stations were selected to illustrate the wide range of optical conditions encountered in Lake Biwa.

Table 3. Scattering and scattering to absorption ratios of sampling sites in Lake Biwa. Scattering coefficient at 440 nm ($b(440)$ m^{-1}), exponent expressing the spectral dependency of $b(\lambda)$ (n), b/a ratios at 555 nm ($b/a(555)$), 440 nm ($b/a(440)$), 380 nm ($b/a(380)$), 340 nm ($b/a(340)$), and 320 nm ($b/a(320)$). Pure water values are included in $a(\lambda)$ and $b(\lambda)$.

Site	$b(440)$	n	$b/a(555)$	$b/a(440)$	$b/a(380)$	$b/a(340)$	$b/a(320)$
North Basin stations							
Nagahama	3.81	0.50	13.8	3.8	1.8	1.5	1.3
EW2	1.15	0.72	8.1	3.3	1.6	1.2	1.0
EW4	0.92	0.75	7.1	3.3	1.4	1.0	0.9
EW6	0.88	0.83	7.1	3.7	2.1	1.3	1.2
EW8	1.06	0.76	7.4	3.7	1.8	1.2	1.1
NS1	1.09	0.73	7.1	3.4	2.5	1.7	1.3
NS3	0.96	0.78	6.9	3.6	2.2	1.6	1.1
NS5	1.00	0.76	7.0	3.5	1.9	1.3	1.0
NS7	1.05	0.77	7.8	3.8	2.4	1.7	1.3
South Basin stations							
Akanoi Bay	8.88	0.85	17.6	4.5	1.6	1.3	1.4
NS9	10.94	0.86	33.5	10.5	4.9	4.2	4.6
NS10	2.29	1.06	9.5	3.6	1.8	1.4	1.3
HamaOtsu	2.29	0.72	10.2	3.8	1.8	1.3	1.1

of a at all PAR wavelengths. Station NS9 (Fig. 3C) was characterized by a large amount of suspended sediment, which caused the water to appear milky; a values at this site rose to 2 m^{-1} at 400 nm. An exception to this close agreement was at Akanoi Bay (Fig. 3D); the absorption values determined there using the AC-9 were 35–57% lower than spectrophotometric measurements. This station showed the highest Chl a concentration and a_{CDOM} (Table 2), and the highest absorption coefficient. The small overestimation of a measured spectrophotometrically at the shorter wavelength of PAR (Fig. 3A–D) was observed at most stations. The relative difference between the two estimates of $a(412)$ was not correlated with $a_{spec}(412)$ ($r = 0.51$, $P = 0.078$) nor with $b/a(412)$ ($r = 0.15$, $P = 0.615$).

PAR scattering at specific wavelengths—The b values, calculated by difference from c and a measured using the AC-9, are illustrated by data from the four contrasting sites presented in Fig. 3. The scattering coefficients varied by more than one order of magnitude among stations (Fig. 3, Table 3) and were strongly correlated with TSS (at 440 nm, $r^2 = +0.994$). At all stations, b decreased approximately linearly with increasing wavelength. The exponent n of the λ^{-n} function varied from 0.50 to 1.06 (mean 0.78; Table 3); n was uncorrelated with either $b(440)$ or TSS. The maximum b/a ratio (incorporating the pure water values for both parameters) was at 555 nm and varied from 6.9 to 33.5; at 440 nm, b/a varied from 3.3 to 10.5 (Table 3).

PAR diffuse attenuation—K_d(PAR) varied from 0.28 to 1.94 m^{-1} among the sampled stations, which translate into euphotic depths (1%) of 2.4 to 16.4 m. A $r^2 > 0.97$ was observed for all computations of K_d(PAR) from the slope of the natural logarithm of $E_d(z, \text{PAR})$ versus depth. Figure 4 shows plots of natural logarithm of $E_d(z, \lambda)$ (normalized to incident irradiance) versus depth at a turbid site (NS9) and a clear station (EW6). At both stations, there was a tendency for K_d(PAR) to decrease with increasing depth; this decrease was observed at nine of the 13 stations. The magnitude of this decrease was estimated by calculating K_d(PAR) separately for the upper and lower portion of each profile. At the stations where a decrease was observed, K_d(PAR) of the lower portion of the profile was 6–27% lower than that of the upper portion. The magnitude of the decrease was not correlated with $b(440)$ or with the b/a ratio at 440 nm.

Modeled PAR diffuse attenuation: K_{dav}—There was a large variation among stations in the shape and absolute values of $K_{dav}(\lambda)$ modeled from Kirk's equation using AC-9 estimates of a and b (Fig. 5). At the clear stations of the North Basin, the variability was relatively small and the highest $K_{dav}(\lambda)$ was at the red end of the spectrum. The stations in the South Basin and the inshore station Nagahama showed much higher attenuation and maximum $K_{dav}(\lambda)$ at the blue end of the spectrum. There was good correspondence between measured K_d(PAR) and the values of $K_{dav}(\lambda)$ integrated over the PAR range with a $r^2 = 0.998$ between the two estimates (Fig. 6A). However, the model systematically underestimated K_d(PAR) by 15–41% (mean 27%), with the highest underestimation at high K_d(PAR) (Fig. 6B). Given the significant difference between spectrophotometric and AC-9 estimates of a at Sta. Akanoi Bay (Fig. 3D), calculations were also made using the spectrophotometric estimates. Using a_{spec} to calculate b from $c_{AC\text{-}9}$ decreased b by 2–17% and decreased the spectral dependency from $n = 0.85$ to $n = 0.54$. K_{dav} modeled using a_{spec} and these values for b increased K_{dav}(PAR) to 1.56 m^{-1}, which is in better agreement with the measured K_d(PAR) (Fig. 6). The dependence of $G(\mu_0)$ on the $\beta(\theta)$ used in the Monte Carlo simulation had little effect on the modeled K_{dav}(PAR) as evidenced by the small error bars in Fig. 6A.

On average, absorption and scattering by pure water, absorption by CDOM, absorption by particles, and particle scattering contributed 17, 23, 29, and 31%, respectively, to K_{dav}(PAR) (Fig. 7). The contribution of particle scattering varied little among stations, from 26 to 31%, except at stations Akanoi Bay, Nagahama, and NS9 (the three stations with TSS > 5 mg L^{-1}) where particle scattering contribution

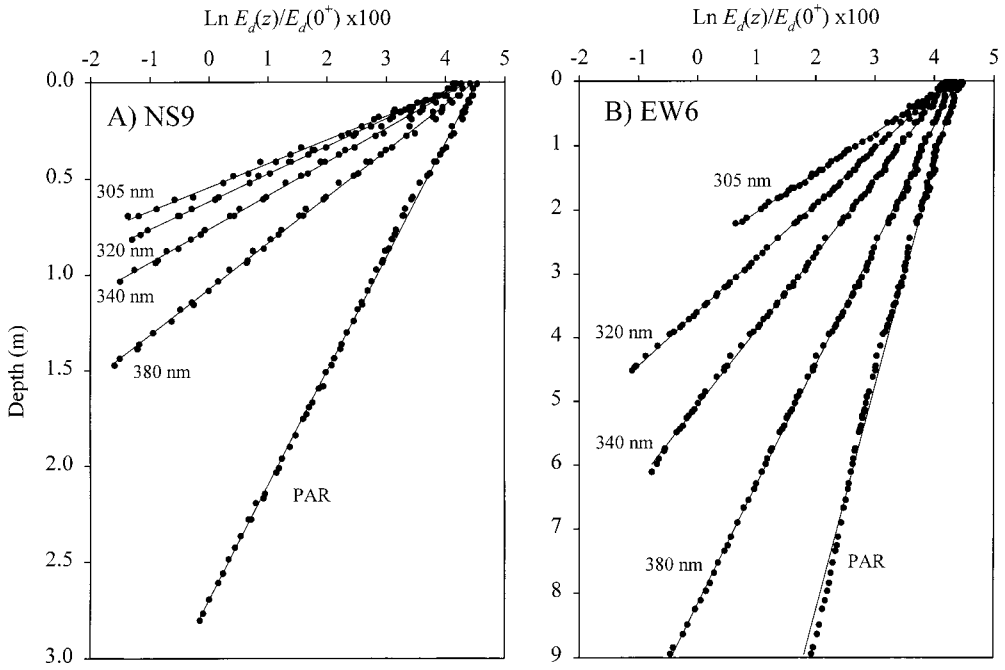

Fig. 4. Profiles of $E_d(z)$ as percent of $E_d(0^+)$ measured using a PUV radiometer (A) at Sta. NS9; and (B) at Sta. EW6.

was 33, 37, and 50%, respectively. CDOM absorption contributed 10–36% to K_{dav}(PAR), and particulate absorption contribution varied from 16 to 43%. The contribution of pure water absorption and scattering varied from 8 to 21%, with the highest contribution at stations with lowest K_{dav}(PAR).

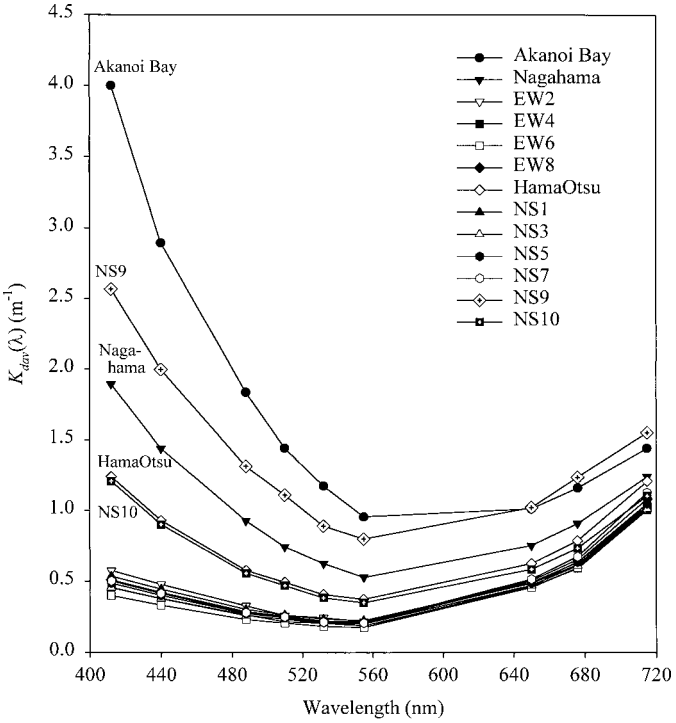

Fig. 5. Spectral $K_{dav}(\lambda)$ in the range 412–715 nm modeled from Kirk's equation using AC-9 estimates of *a* and *b*.

UV absorption and scattering—Values of a_{CDOM} increased exponentially with decreasing wavelength with a slope *S* varying from 0.012 to 0.023 nm^{-1} (Table 2), while a_p attained its maximum at 370–380 nm and decreased slightly at shorter wavelengths. At most stations a_{spec}(UV) increased approximately exponentially with decreasing wavelength (Fig. 3A,B), reflecting the predominant influence of CDOM absorption. However, at stations NS9 and Akanoi Bay (Fig. 3C,D), the larger influence of a_p caused a_{spec} to level off at ~370 nm. Both *a* and *b* increased with decreasing wavelength at all sites; however, the increase of *a* was more or less exponential, whereas the increase of *b* was linear (*see Fig. 3*). Extrapolating *b* into the UV and using *a* from the spectrophotometric determination allowed an estimate of *b*/*a* in the UV waveband. The ratio *b*/*a* varied from 1.4 to 4.9 at 380 nm, from 1.0 to 4.2 at 340 nm, and from 0.9 to 4.6 at 320 nm (Table 3).

UV diffuse attenuation—More than one order of magnitude variation in UV attenuation was observed among the stations. The 1% depth of 320 nm UV was only 0.3 m in Akanoi Bay but reached 3.9 m in the North Basin. As shown on Fig. 4, there was relatively little variation of K_d(UV) with depth. Nevertheless, a detailed analysis similar to that made for PAR showed that increase of K_d at 320, 340, or 380 nm was observed 22 times out of 39, with a maximum increase of 17%. The magnitude of this change of $K_d(\lambda)$ with depth was not correlated with *b*(440) or with the ratio *b*/*a* at 440 nm.

K_d(320) and K_d(380) were strongly correlated with a_{CDOM}, Chl *a*, and TSS (Fig. 8); correlation coefficients for K_d(305) and K_d(340) were very similar to those shown on Fig. 8. While a_{CDOM}(320) and Chl *a* varied by a factor 8 and 5,

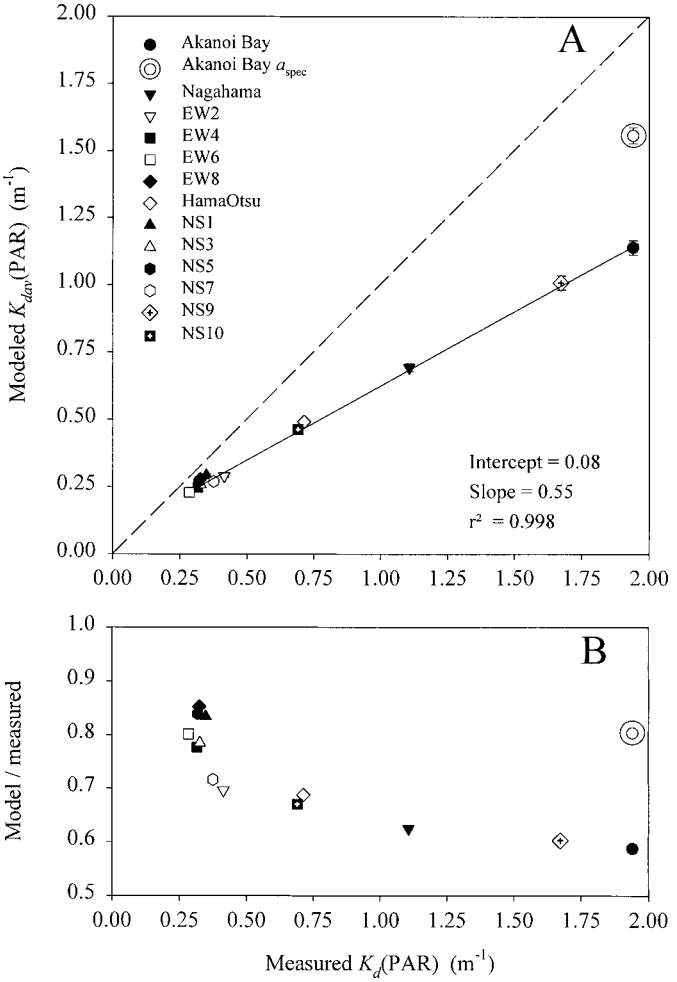

Fig. 6. (A) Relationship between measured and modeled K_{dav}(PAR). Error bars on modeled K_{dav} are the SD values for means resulting from computations using three different relationships between $G(\mu_0)$ and μ_0 (*see Methods*). (B) Ratio of modeled K_{dav}(PAR) to measured K_d(PAR) as a function of K_d(PAR). At Sta. Akanoi Bay, K_{dav} was also modeled using the spectrophotometric estimate of a (a_{spec}).

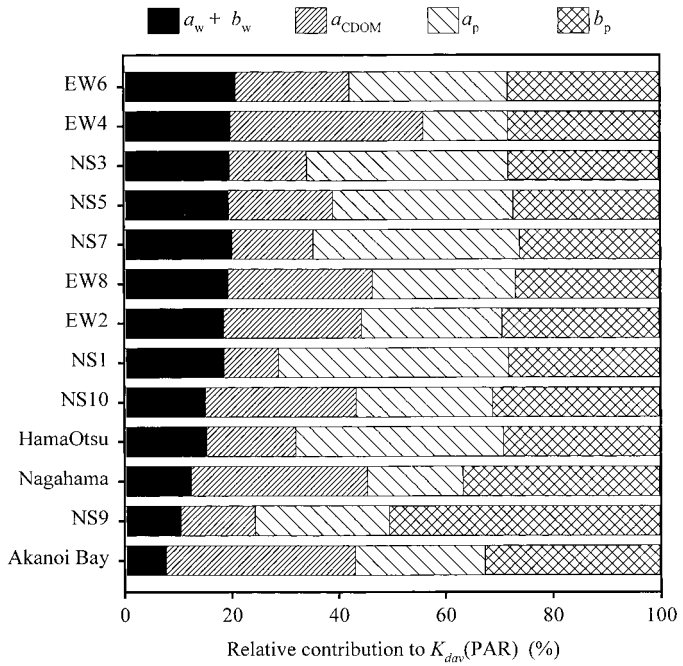

Fig. 7. Relative contribution of absorption and scattering by pure water, absorption by CDOM, absorption by particles, and particle scattering to K_{dav}(PAR) modeled using Kirk's equation. The stations are arranged by increasing K_{dav}(PAR). a_{CDOM} was subtracted from the AC-9 estimates of a to partition dissolved and particulate organic matter contributions. At Sta. Akanoi Bay, the relative contribution was calculated using the spectrophotometric estimates of a.

respectively, TSS varied by a factor 18 among the stations (Table 2). The intercorrelations among these variables limit the use of multivariate analysis in an attempt to identify the best combination of controlling variables. There was substantial difference between measured K_d and K_d estimated from a_{CDOM} using the models of Morris et al. (1995); the mean difference between modeled and measured K_d was 26%, 15%, 18%, and 49% at 305, 320, 340, and 380 nm, respectively (Fig. 8A,D). At the turbid station NS9, Morris et al. models underestimated K_d by 32–51%. K_d(320) calculated from a_{CDOM}(320) using the relationship found for alpine lakes by Laurion et al. (2000) underestimated the measured value by 20% on average and by 60% at Sta. NS9 (Fig. 8A). Further details regarding the deviation between measured K_d(UV) in Lake Biwa and values predicted from correlative models are given in Vincent et al. (2001).

Modeled diffuse attenuation: K_{dav}(380)—At 380 nm, model III taking into account both scattering and total absorption gave an extremely close correspondence to the measured irradiance attenuation, with a r^2 of 0.994 and a relationship close to 1 : 1 (Fig. 9A, Table 4). However, the model tended to overestimate K_d at some stations showing low attenuation. On average, absorption by CDOM and water only (model I) was responsible for 43% of the attenuation (as given by the slope of the linear regression of modeled vs. measured K_{dav}(380), Table 4). Inclusion of a_p in the model (model II) greatly increased the model performance, the modeled K_{dav} being on average 86% of the measured K_d. Neglecting the contribution of particle scattering thus caused about 14% underestimation of K_d(380).

Modeled diffuse attenuation: K_{dav}(340)—At 340 nm, the model accuracy was slightly less than at 380 nm. As for longer wavelength, the inclusion of scattering and a_p gave a much better fit ($r^2 = +0.996$) and a relationship closer to 1 : 1 than obtained with model I considering only CDOM and water absorption (Fig. 9B, Table 4). The relative contributions of pure water, a_{CDOM}, a_p, and particle scattering to UV attenuation were examined by partitioning the modeled K_{dav}(340) between each component (Fig. 10). CDOM absorption was the most important factor; on average it was responsible for 66% of the modeled K_{dav}(340), although its contribution was as low as 40% at Sta. NS9. Particulate absorption also had a significant impact on K_{dav}(340), with a contribution that varied from 13 to 36% (mean 21%). The contribution from pure water was small, from 0.1 to 1.5%.

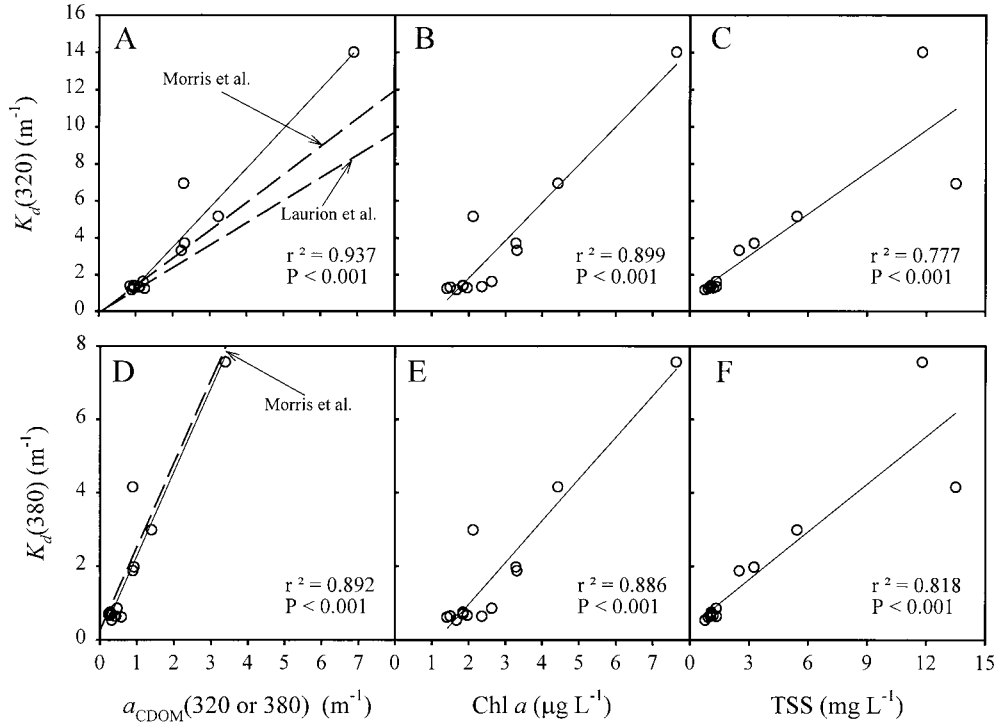

Fig. 8. Correlation between measured $K_d(\lambda)$ in the UV waveband and a_{CDOM}(320 or 380), chlorophyll *a* concentration, and total suspended solids (TSS). (A)–(C) 320 nm; (D)–(F) 380 nm. The dotted lines in (A) and (D) illustrate the results of correlative models of Morris et al (1995) and Laurion et al. (2000) relating K_d to a_{CDOM}.

The contribution of particle scattering to $K_{dav}(340)$ varied from 8 to 13%, except at Sta. NS9 where it reached 24%.

Modeled diffuse attenuation: $K_{dav}(320)$—At 320 nm, there was again a high correlation between modeled K_{dav} and measured K_d ($r^2 = +0.990$); however, the model estimates were on average 31% lower than the measured values (Fig. 9C, Table 4). Absorption by CDOM and water (model I) was responsible on average for 70% of the attenuation, while the contribution of a_p was ~10% (Table 4). Inclusion of particle scattering improved the model performance by about 20%.

Discussion

In general, we found a strong concordance between K_{dav}(PAR) and K_{dav}(UV) determined using the Eq. 2 model and the diffuse attenuation coefficients obtained from in situ measurements. Some difference between the two sets of values is to be expected given the various sources of error associated with the measurements. For example, the increase of $K_d(\lambda)$ with depth caused by modification of the angular distribution of irradiance and the resultant departure from Beer's Law can induce errors in estimating $K_d(\lambda)$ of the order of 10–20% (Gordon 1989). The spectral narrowing of PAR with depth causes K_d(PAR) to decrease with depth (Kirk 1994*b*), although this effect may partly counteract the previous one. The shading by the ship affecting the diffuse component of global irradiance may also cause a measurement error in K_d, since this shading is likely to vary with depth. Over the depth interval considered (from the surface to z_{eu}), the variations of K_d(UV) with depth were generally small and did not give strong support to the results of Monte Carlo simulations that predict an increase of $K_d(\lambda)$ with depth, especially under conditions of high scattering and high SZA (Gordon 1989). Station NS9 (Fig. 4A) displayed the highest scattering, and the irradiance profiles were made at SZA = 42°; however, even at this station, K_d(UV) was maximal near the surface. Small variations of incident irradiance during profiling or slight changes in the IOPs through the water column, together with the shading from the ship, appeared to have a more pronounced influence on the variations of $K_d(\lambda)$ with depth than changes in the angular distribution of irradiance. Decrease of K_d(PAR) with depth associated with the spectral narrowing of PAR was observed at most stations. Because more that 1% of subsurface PAR remained at the maximum depth considered in the K_d(PAR) determination, our measured K_d(PAR) should slightly overestimate the mean K_d through the euphotic zone. Furthermore, the method used to integrate $K_{dav}(\lambda)$ over the PAR waveband (Eq. 4) only takes into account the variations of spectral $E_d(\lambda)$ with depth, neglecting variations of the angular distribution of the irradiance; this should tend to underestimate modeled K_{dav}(PAR). Combined, these two factors may partly explain the discrepancy between modeled and measured values (Fig. 6). This is supported by the closer agreement (slope of measured vs. modeled values closer to 1) found at discrete UV wavelengths (Fig. 9, Table 4).

The measured IOPs used to model $K_{dav}(\lambda)$ are also subject

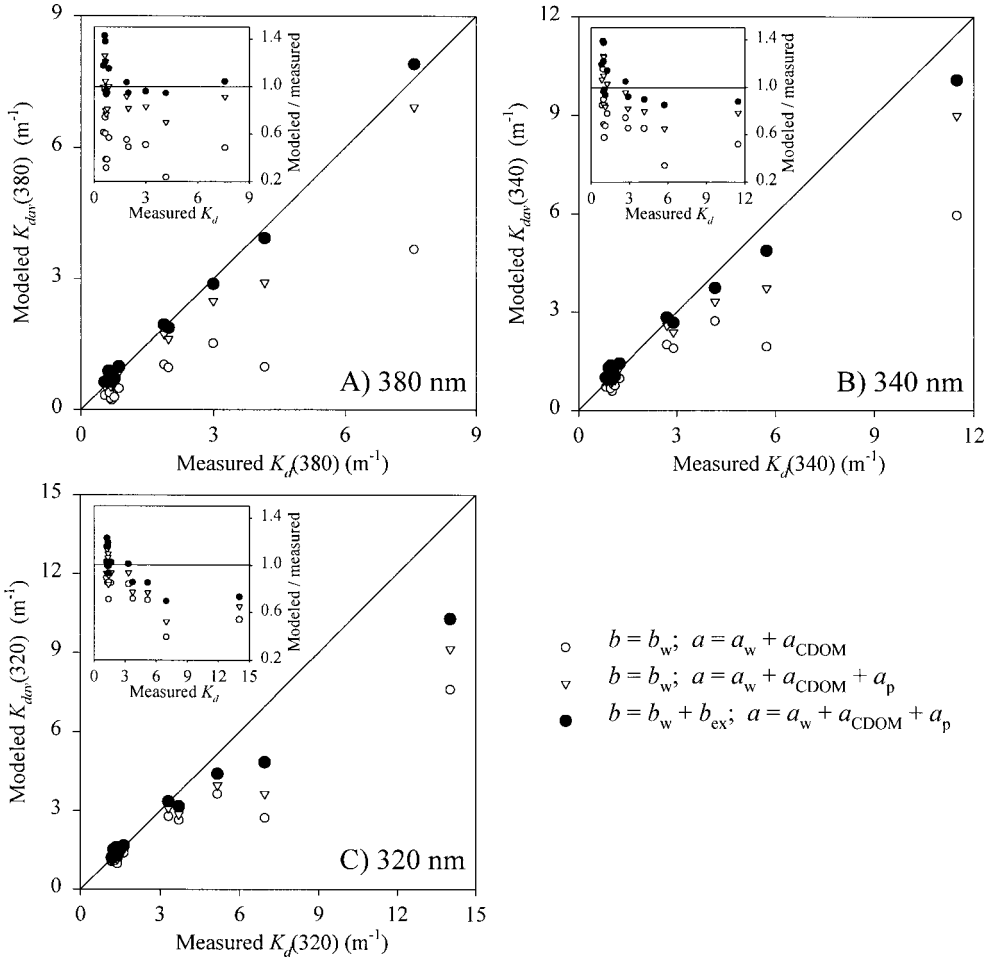

Fig. 9. Relationship between measured $K_d(\lambda)$ and $K_{dav}(\lambda)$ modeled under three assumptions (*see Methods*). (A) 380 nm; (B) 340 nm; and (C) 320 nm. The inserts show the ratio of modeled to measured values as a function of measured $K_d(\lambda)$.

to error. The rated accuracy of the a and c measurements of the AC-9 is 0.005 m^{-1}. However, the actual error on a and b is likely to be much greater due to uncertainties regarding the correction for the scattering loss of the absorption tube (Zaneveld et al. 1994). The discrepancies between a_{spec} and $a_{AC\text{-}9}$ at Akanoi Bay (Fig. 3D) may be due to a significant in situ absorption at 715 nm; in the correction of $a_{AC\text{-}9}$, absorption is assumed to be zero at 715 nm. The assumption of zero absorption at 750 nm for the spectrophotometric a_p determination (Roesler 1998) is more likely to be correct because the filtered volume is adjusted in order to obtain appropriate, relatively low absorbance. If $a_{AC\text{-}9}$ is overcorrected because of significant absorption at 715 nm, the calculated values for b will be overestimated. The better agreement with measured K_d(PAR) found using a_{spec} to calculate K_{dav}(PAR) at Sta. Akanoi Bay suggests such an effect of in situ absorption at 715 nm. However, Roesler (1998) reported excellent agreement between a_p measured using the QFT and the AC-9 estimates for $a_p(\lambda)$ up to ~1.7 m^{-1}. Significant error on the spectrophotometric measurements of a is also expected and would affect the modeled K_{dav}(UV). Appropriate values for the pathlength amplification factor used to correct the particulate absorption measured using the QFT are still under debate (reviewed in Lohrenz 2000). The error on a_p determined using the QFT is typically 15–25% (Lohrenz 2000). In the UV waveband, a_p estimates are less accurate and more subject to modification of the optical properties of the particles during storage (Sosik 1999). Slight changes of absorption properties of our samples are likely, given that immediate analysis or freezing at −80°C was lo-

Table 4. Slope and correlation coefficient of the linear regression of modeled K_{dav}(UV) versus measured K_d(UV) for the three models. Model I considers only scattering by water and absorption by CDOM and water, Model II considers scattering by water and total absorption (particles + CDOM + water), and Model III takes into account total absorption and scattering.

	Model I		Model II		Model III	
λ	Slope	r^2	Slope	r^2	Slope	r^2
320 nm	0.48	0.938	0.55	0.970	0.69	0.990
340 nm	0.46	0.930	0.73	0.984	0.84	0.996
380 nm	0.43	0.896	0.86	0.978	1.01	0.994

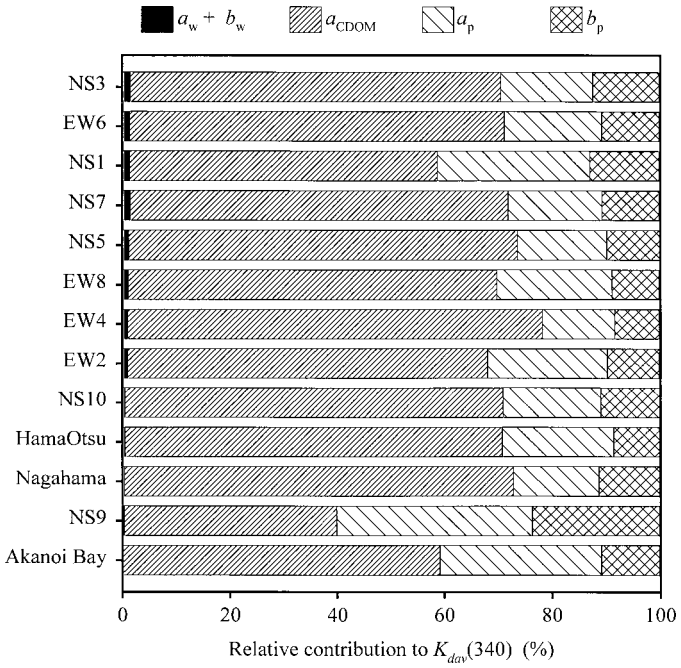

Fig. 10. Relative contribution of absorption and scattering by pure water, absorption by CDOM, absorption by particles, and particle scattering to $K_{dav}(340)$ modeled using Kirk's equation. The stations are arranged by increasing $K_{dav}(340)$.

gistically impossible (cf. Sosik 1999). Extrapolation of a_{CDOM} measured in one λ range to another can induce significant error due to changes of the slope parameter S across the spectrum (Markager and Vincent 2000). Given all these uncertainties, the agreement between a measured using the AC-9 and from spectrophotometry seems highly satisfactory. For the modeling of $K_{dav}(UV)$, b was extrapolated into the UV from measurements in the visible. The extrapolation of b into the UV is more likely to be in error at 320 nm than at 380 nm, since 320 nm is farther from the range of the actual measurements and because the λ^{-n} relationship found in PAR is more likely to break down at shorter wavelengths. Any error in the a_w and b_w estimates that we adopted will also affect the modeled K_{dav} values. The commonly used values of Smith and Baker (1981) are known to represent an upper limit for $a_w(UV)$; for this reason we used the values proposed by Buiteveld et al. (1994), which are ~4 times lower than those of Smith and Baker (1981) and in better agreement with the values of Pope and Fry (1997) that are used in the PAR range.

One potential source of error when applying Eq. 2 to UV irradiance is the strong contribution from the diffuse sky component. In Kirk's Monte Carlo simulation, the irradiance was assumed to consist of a stream of parallel photons. However, results from Morel and Loisel (1998) based on Monte Carlo simulations that include the sky irradiance (their eqs. 20 and 21) are in excellent agreement with those found using Kirk's equation; $K_{dav}(PAR)$ modeled using Morel and Loisel (1998) equations for an atmosphere optical thickness due to aerosols of 0.2 was within 0.5% of values given by Kirk's equation. As the irradiance becomes more diffuse, the variations of $K_d(\lambda)$ with sun angle are smoothed, and for a sun close to zenith μ_0 should be slightly smaller than predicted from SZA using Snell's Law. Kirk (1984), using the $\beta(\theta)$ from San Diego Harbor, found for a standard overcast sky a value for μ_0 of 0.856 and $G(\mu_0) = 0.162$. $K_{dav}(340)$ modeled using these values differed on average by 4.5% from the values modeled using Eqs. 2 and 3. This suggests that the model is relatively insensitive to variations in the relative contributions from direct sun and diffuse sky irradiances.

There was a general tendency for the modeled K_{dav} to increasingly underestimate the measured K_d as K_d increased (Fig. 6 and Fig. 9). Although a combination of the abovementioned errors may explain this result, it cannot be ruled out that a systematic deviation of Kirk's model was responsible. However, given the complexity of radiative transfer in natural waters, Kirk's equation relating K_{dav} to a, b, and μ_0 is remarkably simple, and our results show that in general it provides a good fit to measured data. This model is also a useful tool to assess the relative contribution of a and b to UV attenuation. The Lake Biwa aquatic environment shows a wide range of b/a ratios and is thus particularly well suited to examine the relative contribution of scattering and absorption to diffuse attenuation of UV.

The increase of b with decreasing wavelength measured in this study contrasts with the lack of spectral dependence of b measured using an AC-9 by Roesler and Zaneveld (1994) in East Sound, Washington, and by Pegau et al. (1999) in the case I waters of the Gulf of California. However, Pegau et al. (1999) also found b to increase approximately linearly with decreasing wavelength in some circumstances in case I waters and in case II waters of the Gulf of California where suspended sediments dominated the optical signal. In the latter case, the n exponent of the λ^{-n} relationship was ~0.5. In Lake Biwa, the exponent varied from 0.50 to 1.06 (mean 0.78). There is some evidence that in particle-dominated natural waters, the value of b increases with decreasing wavelengths (Morel and Loisel 1998; Haltrin 1999), and in optical models the spectral dependence of b is generally expressed by λ^{-n} (e.g., Haltrin 1999). When the size distribution function for the particles obeys a Junge law with exponent -4, which is thought to be representative for the ''detrital'' (nonphytoplankton) fraction of the particle population of most natural waters, the particle scattering has been shown to vary approximately with λ^{-1} (*see* Morel 1988). Moreover, Ahn et al. (1992) found that the experimental and theoretical efficiency factor for scattering by the picocyanobacteria *Synechococcus* sp., *Synechocystis* sp., and *Anacystis marina* increased with decreasing wavelength with a slope $\sim\lambda^{-2}$. However, they found no systematic increase of scattering efficiency with decreasing wavelength for larger algal species.

While most correlative models published to date (Scully and Lean 1994; Morris et al. 1995; Laurion et al. 1997; Vincent et al. 1998) found UV attenuation to depend essentially on dissolved organic matter absorption, our results from Lake Biwa show that particulate organic matter can contribute significantly to UV attenuation. The Lake Biwa waters are characterized by relatively low CDOM absorptivity. In these circumstances particulate absorption in the UV plays a significant role in UV attenuation; a_p represented up to 37% of modeled $K_{dav}(340)$ (Fig. 10). Since photosynthetic

pigments (carotenoids, chlorophylls) generally show little UV absorption, the UV particulate absorption is likely to be associated with other cellular components of autotrophic and heterotrophic plankton and to detrital organic matter. Some cyanobacteria occurring in Lake Biwa appear to contain mycosporine-like amino acids (J.J. Frenette et al. unpubl. data), and these compounds may also contribute to the particulate absorption (cf. Whitehead and Vernet 2000). However, the a_p spectra measured during the present study showed no evidence of significant absorption peaks ascribable to these UV-screening compounds. Inorganic particles may also contribute to absorption, although this effect is poorly understood and difficult to determine experimentally. Bukata et al. (1995) and Bowers et al. (1998) suggested that inorganic particles display elevated absorption in the range ~630–700 nm. Such spectral absorption is not accounted for in the AC-9 absorption correction technique and would cause an abrupt increase in b (obtained by difference from c) over this range. However, the form of the spectral b curves for Lake Biwa (Fig. 3) do not indicate any such effect. Seasonal variations in a_{CDOM} in Lake Biwa have yet to be studied. Given the high irradiance level and relatively shallow stratification, it is likely that the CDOM was partially photobleached at the period of sampling, in late summer. The high S value observed at most stations (Table 2) might be indicative of such photodegraded CDOM (Vodacek et al. 1997).

Organic and mineral particles also contribute to scattering, thereby increasing the contribution of seston to the UV-attenuation coefficients. The scattering contribution to $K_{\mathrm{dav}}(\mathrm{UV})$ was relatively small at the stations sampled in Lake Biwa; at 340 nm scattering increased K_{dav} from 8 to 24% above the value dictated by absorption by water, CDOM, and particles (Fig. 10). Given the linear relationship between b and λ and the nonlinear relationship between a and λ (Fig. 3), the attenuation coefficient was increasingly dominated by absorption with decreasing λ (compare Fig. 7 and Fig. 10). As evidenced by the shape of $\beta(\theta)$, most particle scattering occurs at small forward angles (Gordon 1989). Thus, a large increase of b is needed to increase significantly the mean pathlength of the photons and thereby increase K_d. Our results provide quantitative support for the suggestion by Smith et al. (1999) that at high suspended solid concentrations scattering makes a large contribution to $K_d(\mathrm{UV})$; in Lake Erie the TSS ranged up to 124 mg L^{-1} (nine times greater than at Sta. NS9 in Lake Biwa) and contributed to values of $K_d(320)$ up to 60 m^{-1}.

The relative contribution of water, dissolved matter, and particulate matter to the total UV-absorption coefficient will influence the extent of photochemical and photobiological effects. During blooms in Lake Biwa, phytoplankton and associated particles (not CDOM) might absorb most of the UV. In these circumstances, the anticipated photodamaging effects of UV would be larger than for a water body receiving the same UV irradiance but in which CDOM absorption dominates UV attenuation. Moreover, it has been shown that local increase in scattering (e.g., nepheloid layer) functions as an optical energy trap by increasing the mean light path through the layer (Stavn 1982). The scattering associated with such particles increases the mean pathlength of UV photons, causing an increased probability of photobiological or photochemical effects.

Detailed in situ profiles of spectral absorption and attenuation measured using the AC-9 (e.g., Fig. 1) may help to improve significantly our understanding of optics of natural waters. A precise understanding of IOPs is essential for inverting remotely sensed data to obtain water quality parameters such as chlorophyll *a*, suspended solids, or DOC. The relatively large size and deep waters (thus absence of bottom reflectance) of the North Basin of the Lake Biwa, together with the relatively low a_{CDOM}, may allow remote sensing of water color in the near future, and this would help forecasting nuisance bloom development.

There are many indications that climate change–related modifications of CDOM input to aquatic ecosystems are likely to affect biological UV exposure in the underwater environment to a greater extent than ozone depletion (Gibson et al. 2000; Pienitz and Vincent 2000). Our results suggest that modifications of particle input may also significantly affect UV exposure. Climate change may affect the concentration, distribution, and nature of particles in the water column, for example through changes in stream and river runoff, mixing regime, frequency, or intensity of storm events or, in regions influenced by glaciers and permafrost, inputs of glacial flour and other fine light-scattering sediments. The results presented here show that Kirk's equation is appropriate to the UV waveband and will allow such effects to be modeled and evaluated.

References

AHN, Y.-H., A. BRICAUD, AND A. MOREL. 1992. Light backscattering efficiency and related properties of some phytoplankters. Deep-Sea Res. **39:** 1835–1855.

BOWERS, D. G., S. BOUDJELAS, AND G. E. L. HARKER. 1998. The distribution of fine suspended sediments in the surface waters of the Irish Sea and its relation to tidal stirring. Int. J. Remote Sens. **19:** 2789–2805.

BUITEVELD, H., J. H. M. HAKVOORT, AND M. DONZE. 1994. The optical properties of pure water, p. 174–183. *In* Ocean Optics XIII. Proc. SPIE **2258.**

BUKATA, R. P., J. H. JEROME, K. Y. KONDRATYEV, AND D. V. POZDNYAKOV. 1995. Optical properties and remote sensing of inland and coastal waters. CRC.

GIBSON, J. A. E., W. F. VINCENT, B. NIEKE, AND R. PIENITZ. 2000. Control of biological exposure to UV radiation in the Arctic Ocean: Comparison of the roles of ozone and riverine dissolved organic matter. Arctic **53:** 372–382.

GORDON, H. R. 1989. Can the Lambert-Beer law be applied to the diffuse attenuation coefficient of ocean water? Limnol. Oceanogr. **34:** 1389–1409.

HALTRIN, V. I. 1999. Chlorophyll-based model of seawater optical properties. Appl. Opt. **38:** 6826–6832.

HODOKI, Y., AND Y. WATANABE. 1998. Attenuation of solar ultraviolet radiation in eutrophic freshwater lakes and ponds. Jpn. J. Limnol. **59:** 27–37.

KIRK, J. T. O. 1984. Dependence of relationship between inherent and apparent optical properties of water on solar altitude. Limnol. Oceanogr. **29:** 350–356.

———. 1991. Volume scattering function, average cosines, and the underwater light field. Limnol. Oceanogr. **36:** 455–467.

———. 1994*a*. Characteristics of the light field in highly turbid waters: A Monte Carlo study. Limnol. Oceanogr. **39:** 702–706.

———. 1994*b*. Light and photosynthesis in aquatic ecosystems, 2nd ed. Cambridge Univ. Press.

LAURION, I., M. VENTURA, J. CATALAN, R. PSENNER, AND R. SOMMARUGA. 2000. Attenuation of ultraviolet radiation in mountain lakes: Factors controlling the among- and within-lake variability. Limnol. Oceanogr. **45:** 1274–1288.

———, W. F. VINCENT, AND D. R. S. LEAN. 1997. Underwater ultraviolet radiation: Development of spectral models for Northern high latitude lakes. Photochem. Photobiol. **65:** 107–114.

LOHRENZ, S. E. 2000. A novel theoretical approach to correct for pathlength amplification and variable sampling loading in measurements of particulate spectral absorption by the quantitative filter technique. J. Plankton Res. **22:** 639–657.

MARKAGER, S., AND W. F. VINCENT. 2000. Spectral light attenuation and the absorption of UV and blue light in natural waters. Limnol. Oceanogr. **45:** 642–650.

MOREL, A. 1988. Optical modeling of the upper ocean in relation to its biogenous matter content (case I waters). J. Geophys. Res. **93:** 10749–10768.

———, AND H. LOISEL. 1998. Apparent optical properties of oceanic water: Dependence on the molecular scattering contribution. Appl. Opt. **37:** 4765–4776.

MORRIS, D. P., H. ZAGARESE, C. E. WILLIAMSON, E. G. BALSEIRO, B. R. HARGREAVES, B. MODENUTTI, R. MOELLER, AND C. QUEIMALINOS. 1995. The attenuation of solar UV radiation in lakes and the role of dissolved organic carbon. Limnol. Oceanogr. **40:** 1381–1391.

NUSCH, E. A. 1980. Comparison of different methods for chlorophyll and phaeopigment determination. Arch. Hydrobiol. Beih. **14:** 14–36.

PEGAU, W. S., D. GRAY, AND J. R. V. ZANEVELD. 1997. Absorption and attenuation of visible and near-infrared light in water: Dependence on temperature and salinity. Appl. Opt. **36:** 6035–6046.

———, J. R. V. ZANEVELD, A. H. BARNARD, H. MASKE, S. ÁLVAREZ-BORREGO, R. LARA-LARA, AND R. CERVANTES-DUARTE. 1999. Inherent optical properties in the Gulf of California. Cienc. Mar. **25:** 469–485.

PIENITZ, R., AND W. F. VINCENT. 2000. Effect of climate change relative to ozone depletion on UV exposure in subarctic lakes. Nature **404:** 484–487.

POPE, R. M., AND E. S. FRY. 1997. Absorption spectrum (380–700 nm) of pure water. II. Integrating cavity measurements. Appl. Opt. **36:** 8710–8723.

ROESLER, C. S. 1998. Theoretical and experimental approaches to improve the accuracy of particulate absorption coefficients derived from the quantitative filter technique. Limnol. Oceanogr. **43:** 1649–1660.

———, AND J. R. V. ZANEVELD. 1994. High resolution vertical profiles of spectral absorption, attenuation, and scattering coefficients in highly stratified waters, p. 309–319. *In* Ocean Optics XII. Proc. SPIE **2258.**

SCULLY, N. M., AND D. R. S. LEAN. 1994. The attenuation of ultraviolet radiation in temperate lakes. Arch. Hydrobiol. Beih. **43:** 135–144.

SHOOTER, D., R. J. DAVIES-COLLEY, AND J. T. O. KIRK. 1998. Light absorption and scattering by ocean waters in the vicinity of the Chatham Rise, South Pacific Ocean. Mar. Freshw. Res. **49:** 455–461.

SMITH, R. C., AND K. S. BAKER. 1981. Optical properties of the clearest natural waters (200–800 nm). Appl. Opt. **20:** 177–184.

SMITH, R. E. H., J. A. FURGAL, M. N. CHARLTON, B. M. GREENBERG, V. HIRIART, AND C. MARWOOD. 1999. Attenuation of ultraviolet radiation in a large lake with low dissolved organic matter concentrations. Can. J. Fish. Aquat. Sci. **56:** 1351–1361.

SOSIK, H. M. 1999. Storage of marine particulate samples for light-absorption measurements. Limnol. Oceanogr. **44:** 1139–1141.

STAVN, R. H. 1982. The three-parameter model of the submarine light field: Radiant energy absorption and energy trapping in nepheloid layers. J. Geophys. Res. **87:** 2079–2082.

VINCENT, W. F., M. KUMAGAI, C. BELZILE, K. ISHIKAWA, AND K. HAYAKAWA. IN PRESS. Effects of seston on ultraviolet attenuation in Lake Biwa. Limnology.

———, R. RAE, I. LAURION, C. HOWARD-WILLIAMS, AND J. C. PRISCU. 1998. Transparency of Antarctic ice-covered lakes to solar UV radiation. Limnol. Oceanogr. **43:** 618–624.

VODACEK, A., N. V. BLOUGH, M. D. DEGRANDPRE, E. T. PELTZER, AND R. K. NELSON. 1997. Seasonal variation of CDOM and DOC in the Middle Atlantic Bight: Terrestrial inputs and photooxidation. Limnol. Oceanogr. **42:** 674–686.

WEIDEMANN, A. D., AND T. T. BANNISTER. 1986. Absorption and scattering coefficients in Irondequoit Bay. Limnol. Oceanogr. **31:** 567–583.

WHITEHEAD, K., AND M. VERNET. 2000. Influence of mycosporine-like amino acids (MAAs) on UV absorption by particulate and dissolved organic matter in La Jolla Bay. Limnol. Oceanogr. **45:** 1788–1796.

ZANEVELD, J. R., J. C. KITCHEN, AND C. MOORE. 1994. The scattering error correction of reflecting-tube absorption meters, p. 44–55. *In* Ocean Optics XII. Proc. SPIE **2258.**

Received: 5 March 2001
Accepted: 12 September 2001
Amended: 2 October 2001